RESTRICTED

Copy 105
RM L50E02

NACA RM L50E02

NACA

RESEARCH MEMORANDUM

LOW-SPEED INVESTIGATION OF LEADING-EDGE AND TRAILING-EDGE FLAPS ON A 47.5° SWEPTBACK WING OF ASPECT RATIO 3.4 AT A REYNOLDS NUMBER OF 4.4×10^6

By Jerome Pasamanick and Thomas B. Sellers

Langley Aeronautical Laboratory
Langley Air Force Base, Va.

NATIONAL ADVISORY COMMITTEE FOR AERONAUTICS

WASHINGTON

June 12, 1950

RESTRICTED

NATIONAL ADVISORY COMMITTEE FOR AERONAUTICS

RESEARCH MEMORANDUM

LOW-SPEED INVESTIGATION OF LEADING-EDGE AND TRAILING-EDGE FLAPS ON A 47.5° SWEPTBACK WING OF ASPECT RATIO 3.4 AT A REYNOLDS NUMBER OF 4.4×10^6

By Jerome Pasamanick and Thomas B. Sellers

SUMMARY

An investigation was made in the Langley full-scale tunnel of the low-speed longitudinal characteristics of a 47.5° sweptback wing-fuselage combination (aspect ratio 3.4) with various extensible leading-edge-flap and plain trailing-edge-flap arrangements. For the configuration investigated, a 10-percent-chord, 30-percent-span or 35-percent-span leading-edge flap deflected 135° or 150° produced longitudinal stability over the complete lift-coefficient range. Flaps of larger spans and chords also produced satisfactory longitudinal stability characteristics, but there was no appreciable increase in the maximum-lift increments. The wing with plain trailing-edge flaps produced the largest increment of maximum-lift coefficient (0.17) but resulted in unstable pitching-moment characteristics near the stall. Combining the 10-percent-chord leading-edge flaps and the trailing-edge flap resulted in longitudinal stability for the smallest span flaps investigated.

INTRODUCTION

In numerous investigations it has been shown that the initial flow breakdown over the tip sections of thin highly swept wings results in poor longitudinal stability characteristics and low values of maximum lift. In order to alleviate the early flow breakdown, extensible leading-edge flaps, similar to those investigated in reference 1, have been used as a means for delaying tip stall; but for each wing sweep angle there appears to be a limited range of flap configuration which produces satisfactory stability. In the course of an earlier investigation of a highly swept low-aspect-ratio wing in the Langley full-scale tunnel (reference 2), a few leading-edge-flap configurations indicated that, with a careful selection of leading-edge and trailing-edge flaps, it would be possible to obtain sufficient control of the flow over the wing to produce satisfactory stability and improved lift characteristics of the particular plan form. The results of the investigations of references 3 and 4 also indicate the variable range of flap required to produce longitudinal stability for each particular plan form.

The present paper contains the results of an investigation to determine the effects of leading-edge-flap chord, span, and deflection angle on the aerodynamic characteristics in pitch of a 47.5° sweptback wing-fuselage combination. Results are also included for the model with plain trailing-edge flaps used alone and in combination with the leading-edge flaps. The wing aspect ratio was 3.4, the taper ratio was 0.51, and the airfoil sections were NACA 64_1A112. The average Reynolds number for the tests was 4.4×10^6 and the Mach number was approximately 0.07.

SYMBOLS

C_L	lift coefficient (L/q_oS)
C_D	drag coefficient (D/q_oS)
C_m	pitching-moment coefficient $(M/q_oS\bar{c})$
$\Delta C_{L_{max}}$	increment of maximum-lift coefficient due to flaps
L	lift, pounds
D	drag, pounds
M	pitching moment about the quarter chord of the mean aerodynamic chord; positive when moment tends to increase angle of attack, foot-pounds
S	total wing area, square feet
q_o	free-stream dynamic pressure, pounds per square foot $\left(\frac{1}{2}\rho V_o^2\right)$
ρ	mass density of air, slugs per cubic foot
V_o	free-stream velocity, feet per second
c	wing chord measured perpendicular to quarter-chord line, feet
c'	wing chord measured parallel to plane of symmetry, feet

$\bar{c}$ wing mean aerodynamic chord measured parallel to plane of symmetry, feet $\left(\frac{2}{S}\int_{0}^{b/2} c'^{2}dy\right)$

y distance measured perpendicular to plane of symmetry, feet

b wing span measured perpendicular to plane of symmetry, feet

α angle of attack of wing chord line measured in plane of symmetry, degrees

δ flap deflection angle, degrees

Subscripts:

LE extensible leading-edge flaps

TE plain trailing-edge flaps

MODEL

General dimensions of the model are given in the three-view drawing of figure 1, and figure 2 presents a photograph of the model mounted in the Langley full-scale tunnel. The wing leading-edge sweepback was 47.5°, the aspect ratio was 3.4, the taper ratio was 0.51, and the airfoil sections normal to the quarter-chord line were NACA 64_1A112. The wing panels had no geometric dihedral and no twist and were mounted in a low midwing position at zero incidence on a circular fuselage.

The details of the extensible leading-edge and plain trailing-edge flaps investigated are given in figure 3 and the variable parameters are tabulated in the following table:

Flap	Span (percent b/2)	Chord (percent)	Deflection angle (deg)
Extensible leading edge	30, 35, 40 45, 50, 55, 60	10, 15, 20	120, 135, 150
Plain trailing edge	20.5, 43.0, 65.5, 88	19	20, 40, 60

The chords and deflection angles of the extensible leading-edge flaps were measured from the chord line in a plane parallel to the plane of symmetry. These flaps extended outward to the wing tip and were tangent to the wing surface. The plain trailing-edge flaps extended outward from the 12-percent-semispan station and were deflected normal to the hinge line (81-percent chord measured in a plane perpendicular to the quarter-chord line). For a few exploratory tests the existing leading-edge flap nose was closed by a circular insert faired to the flap contour as shown in figure 3.

TESTS AND RESULTS

The tests were made on the six-component balance system of the Langley full-scale tunnel at a Reynolds number of 4.4×10^6 and a Mach number of approximately 0.07. Data were obtained at zero yaw over a range of angle of attack from small negative angles through the angle for maximum lift.

All the data have been corrected for jet-boundary effects (as determined from the straight-wing method of reference 5), blocking effects, stream alinement, and approximate wing-support interference.

In order to facilitate the discussion of results, the data are arranged in the following order of figures: The plain-wing characteristics are presented in figure 4. The data of the wing with extensible leading-edge flaps, plain trailing-edge flaps, and combinations of both flaps are given in figures 5, 6, and 7, respectively. Summary curves of maximum-lift increments and longitudinal stability characteristics for the different flap arrangements are presented in figures 8 to 10.

DISCUSSION OF RESULTS

Basic longitudinal characteristics.- The maximum-lift coefficient of the plain wing was 0.99 at an angle of attack of 22° (fig. 4). The slope of the lift curve in the low and moderate lift range was essentially linear up to a lift coefficient of approximately 0.75. The results of reference 2 have shown that at the higher lift coefficients a small bubble of separation occurred at the leading edge of the outboard section producing a local increase in lift at the tips and a sudden increase in longitudinal stability. The results presented in figure 4 show the increased longitudinal stability at the higher lift coefficients, but the accompanied local lift increase at the tip sections can not be readily observed from the total-lift curve. At lift coefficients above 0.9 a rapid progression of separation over the leading edge of the outboard sections suddenly reduced the lift and introduced abrupt longitudinal instability.

Extensible leading-edge flaps.- Figure 5 illustrates the effect of varying the leading-edge-flap configurations on the longitudinal characteristics of the model. An analysis of the data indicates that a decrease in drag occurs at moderate and high angles of attack as the flaps are extended inboard because of the delay of leading-edge separation over a greater part of the wing span. The results indicate that, for the swept wing investigated, the extensible leading-edge flaps would not produce large lift increments; but, by suitable combination of flap variables, static longitudinal stability could be obtained throughout the C_L range: The summary curves (fig. 8) show that, for the flap deflection of 120°, longitudinal stability was obtained only for the 10-percent-chord and 15-percent-chord flaps of the smallest spans at the wing tips. For the higher flap deflections of 135° or 150°, longitudinal stability at the stall can be obtained with flaps of larger chords and spans. In general for design and structural simplicity, the 10-percent-chord flaps appear to be the most promising configuration for this plan form inasmuch as satisfactory stability and some increase in maximum lift can be obtained with small spans for each deflection angle investigated.

The maximum value of $\Delta C_{L_{max}}$ obtained was approximately 0.10 (fig. 8). Flap chord and deflection angle had negligible effects on the maximum value of $\Delta C_{L_{max}}$ but did affect the flap span required to obtain this increment. As the flap deflection angle was progressively increased, a smaller flap span was required for the 10-percent-chord and 15-percent-chord flaps.

A few exploratory tests were made with the 10-percent-chord, 135°-deflected flaps with the nose closed (fig. 3) to determine whether the stagnation point had moved sufficiently under the original leading-edge contour with an increase in angle of attack to affect adversely the flow over the flap. The results of these tests were identical to the partial-open-nose-flap results and are not included on the data figures.

Plain trailing-edge flaps.- The longitudinal stability characteristics for all trailing-edge-flap configurations were similar to the plain-wing characteristics. The pitching-moment curves indicated sudden stability followed by an abrupt instability near the maximum lift (fig. 6). An increase in the flap span resulted in an appreciable trim shift which increased further with increasing deflection angle.

The increments of maximum lift due to flap deflection are presented in figure 9 as a function of flap span. The results indicate that varying the deflection angle from 20° to 40° produced the greater maximum-lift increments. A further increase in deflection angle, to 60°, reduced the maximum-lift increments (about -0.02) and greatly reduced the lift-drag ratios throughout the flap-span range (fig. 6). The maximum increment in lift obtained was about 0.17 for the wing with full-span flaps deflected 40°.

Flap combinations.- The variation of maximum-lift increments with the leading-edge flap combined with the trailing-edge flaps is shown in figure 10. The variables held constant for these tests were the leading-edge-flap chord (10 percent) and the trailing-edge-flap deflection angle (40°).

The 30-percent-span leading-edge flaps deflected 135° or 150° in combination with the 43-percent-span trailing-edge flaps were the only configurations tested, which resulted in longitudinal stability near the stall (fig. 7). The increment of maximum lift obtained for these combinations which produced stability at stall was approximately 0.15.

The smaller leading-edge-flap deflection angle produced larger maximum-lift increments for the flap combinations investigated throughout most of the leading-edge-flap-span range (fig. 10). The 65.5-percent-span and 88.0-percent-span trailing-edge flaps in combination with the leading-edge flaps deflected 150° produced constant maximum-lift values for the leading-edge spans investigated.

The drag coefficients of the model for each trailing-edge-flap span were not appreciably affected with variation of leading-edge-flap span. It was previously pointed out that the leading-edge flaps reduced the drag coefficients; however, the drag decrement can not be observed for the model configurations with flap combinations because of the large drag increment produced by the trailing-edge flaps.

SUMMARY OF RESULTS

The results of the investigation in the Langley full-scale tunnel of the effect of flap design parameters on the aerodynamic characteristics of a 47.5° sweptback wing are summarized as follows:

1. For the present plan form, a 10-percent-chord, 30-percent-span or 35-percent-span leading-edge flap deflected 135° or 150° appeared to be the most promising configuration inasmuch as longitudinal stability was obtained throughout the lift-coefficient range. Flaps of larger spans and chords also produced satisfactory longitudinal stability

characteristics, but the maximum-lift increments obtained were not appreciably greater than those for the smaller-span flaps.

2. The plain trailing-edge-flap configurations were longitudinally unstable at the stall. The highest lift increment obtained was 0.17 for the wing with full-span flaps deflected 40°.

3. For the combinations of trailing-edge flaps and 10-percent-chord extensible leading-edge flaps, longitudinal stability was obtained only for the 30-percent-span leading-edge flaps deflected 135° or 150° in combination with the 43-percent-span plain trailing-edge flaps deflected 40°.

Langley Aeronautical Laboratory
National Advisory Committee for Aeronautics
Langley Air Force Base, Va.

REFERENCES

1. Krueger, W.: Systematic Wind-Tunnel Measurements on a Laminar Wing with Nose Flap. NACA TM 1119, 1947.

2. Pasamanick, Jerome, and Sellers, Thomas B.: Full-Scale Investigation of Boundary-Layer Control by Suction through Leading-Edge Slots on a Wing-Fuselage Configuration Having 47.5° Leading-Edge Sweep with and without Flaps. NACA RM L50B15, 1950.

3. Koven, William, and Graham, Robert R.: Wind-Tunnel Investigation of High-Lift and Stall-Control Devices on a 37° Sweptback Wing of Aspect Ratio 6 at High Reynolds Numbers. NACA RM L8D29, 1948.

4. Foster, Gerald V., and Fitzpatrick, James E.: Longitudinal-Stability Investigation of High-Lift and Stall-Control Devices on a 52° Sweptback Wing with and without Fuselage and Horizontal Tail at a Reynolds Number of 6.8×10^{6}. NACA RM L8I08, 1948.

5. Theodorsen, Theodore, and Silverstein, Abe: Experimental Verification of the Theory of Wind-Tunnel Boundary Interference. NACA Rep. 478, 1934.

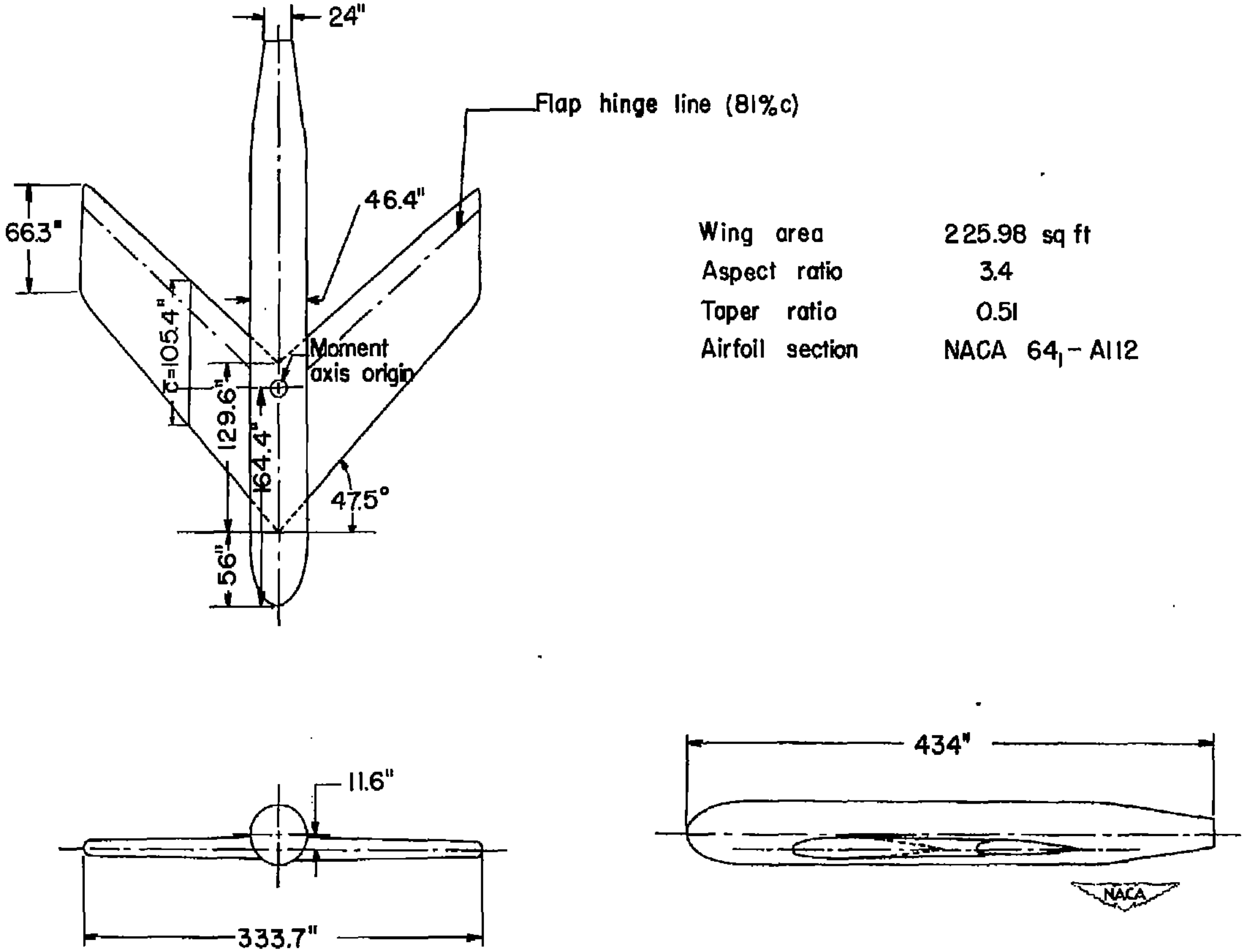

Wing area	225.98 sq ft
Aspect ratio	3.4
Taper ratio	0.51
Airfoil section	NACA 64_1 - A112

Figure 1.—Three-view drawing of a 47.5° sweptback wing-fuselage combination.

Figure 2.- Three-quarter front view of the 47.5° sweptback-wing model mounted in the Langley full-scale tunnel.

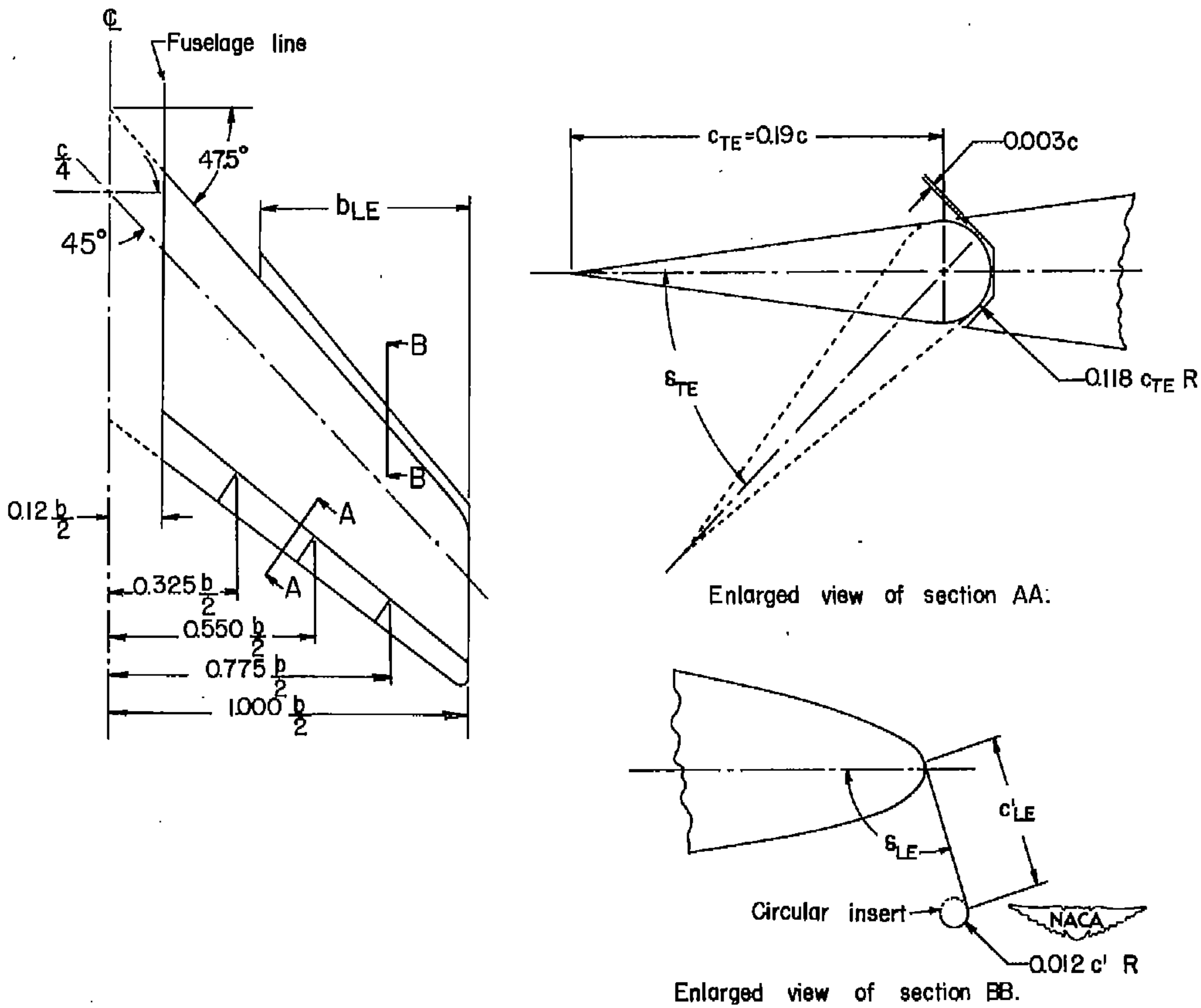

Figure 3.— The location and detail dimensions of extensible leading-edge flaps and plain trailing-edge flaps.

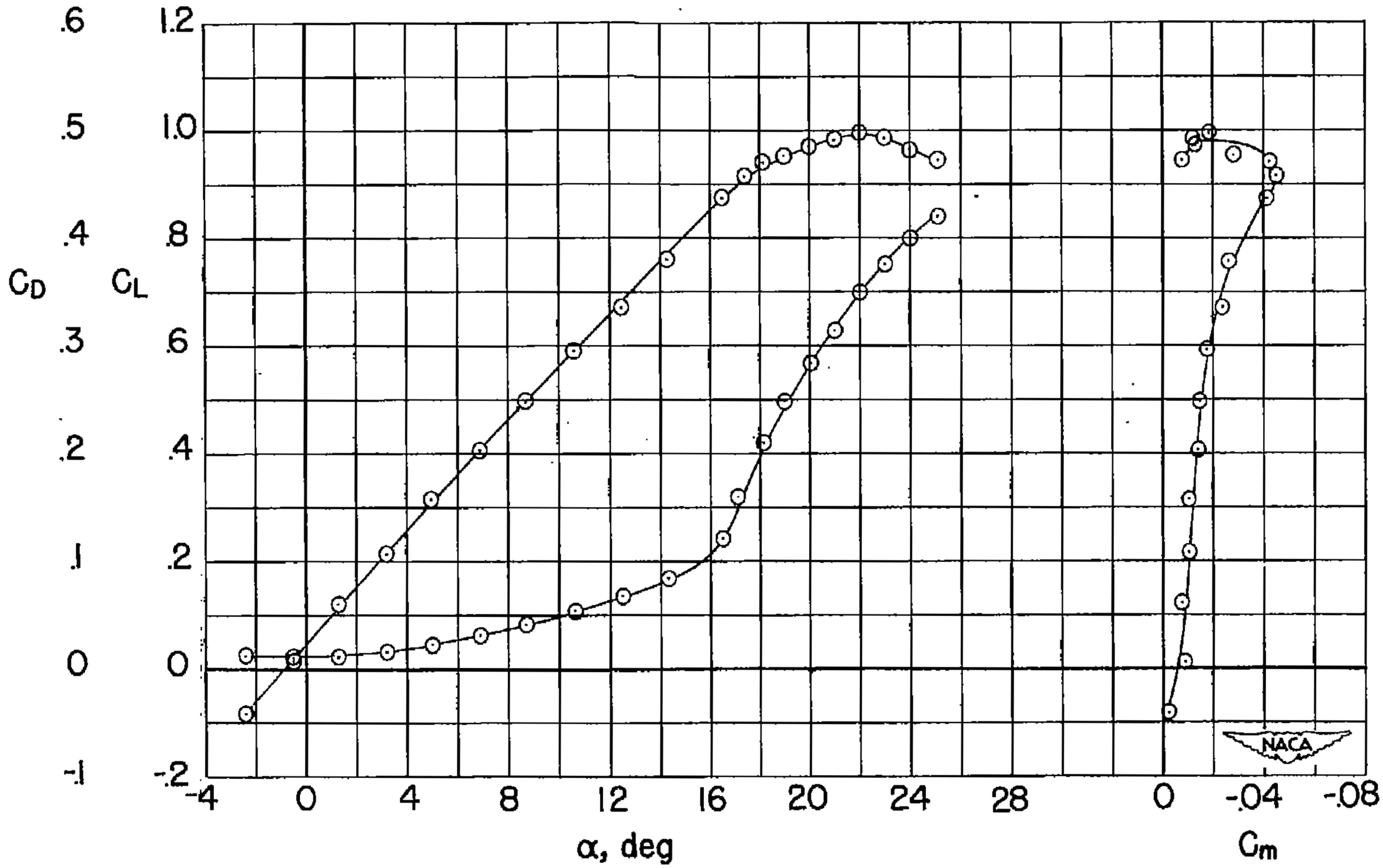

Figure 4.– Aerodynamic characteristics of a 47.5° sweptback wing-fuselage combination. $R = 4.4 \times 10^6$.

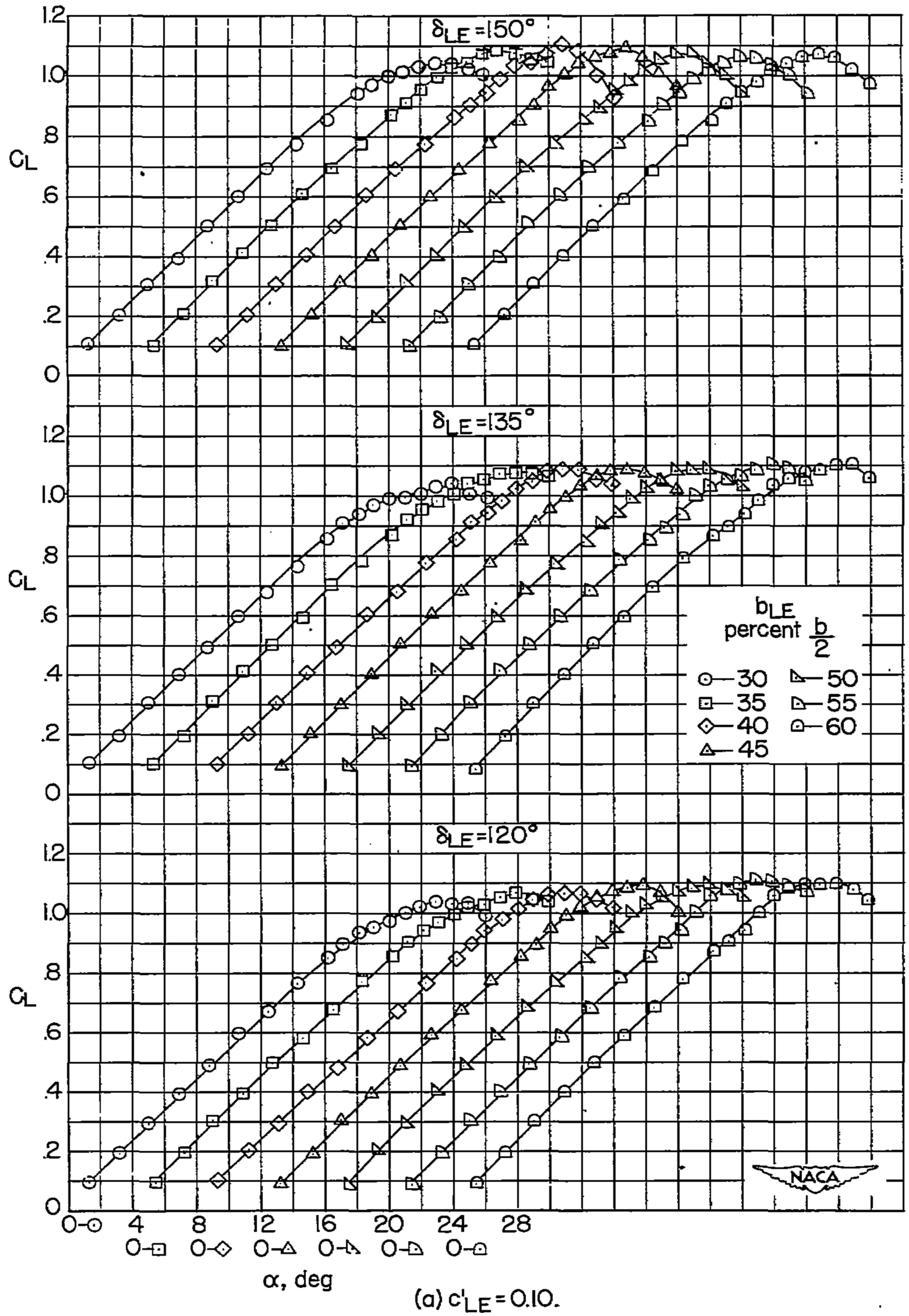

(a) $c'_{LE} = 0.10$.

Figure 5.– Aerodynamic characteristics of a 47.5° sweptback wing-fuselage combination with extensible leading-edge flaps. $R = 4.4 \times 10^6$.

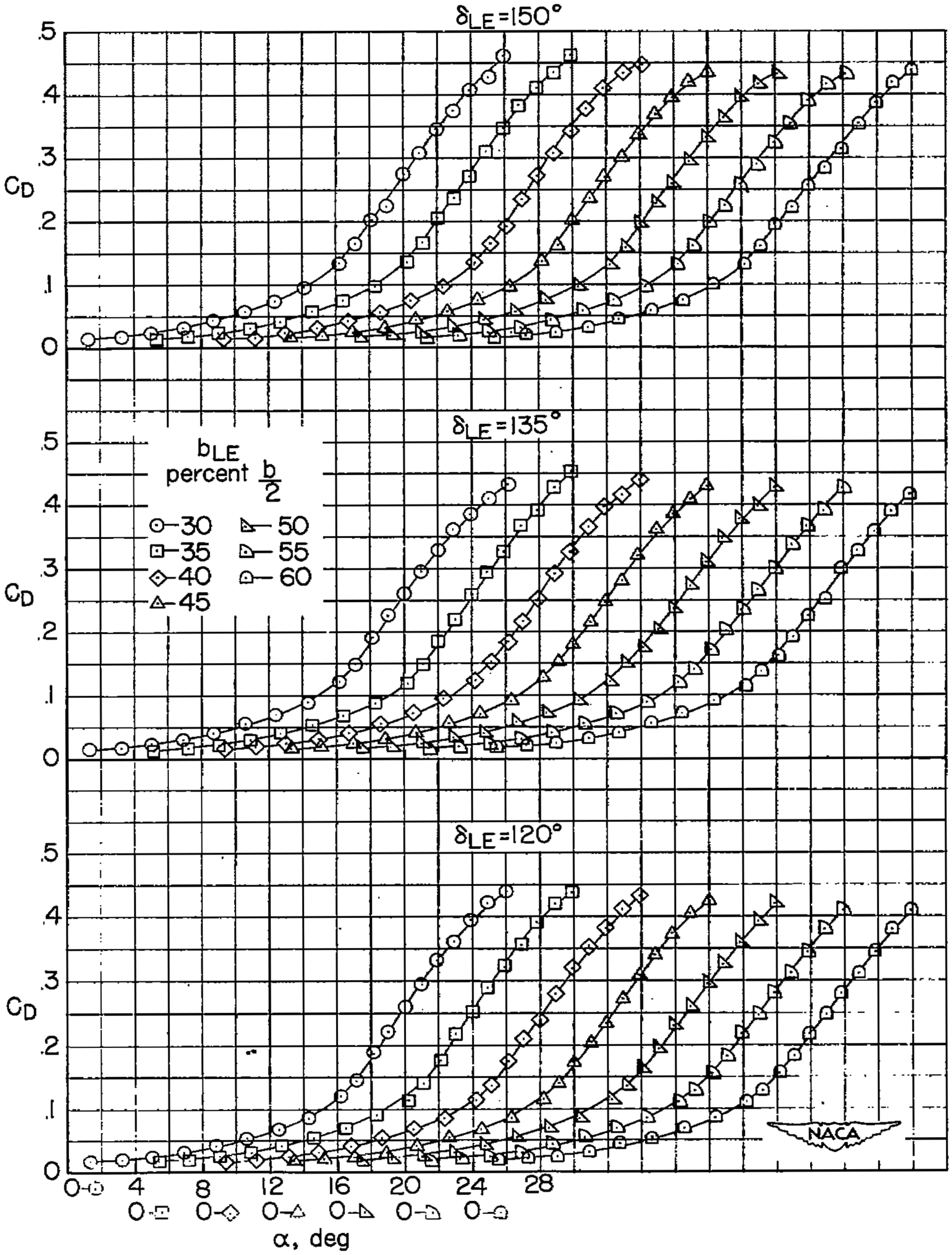

(a) c'_{LE} = 0.10. Continued.

Figure 5.—Continued.

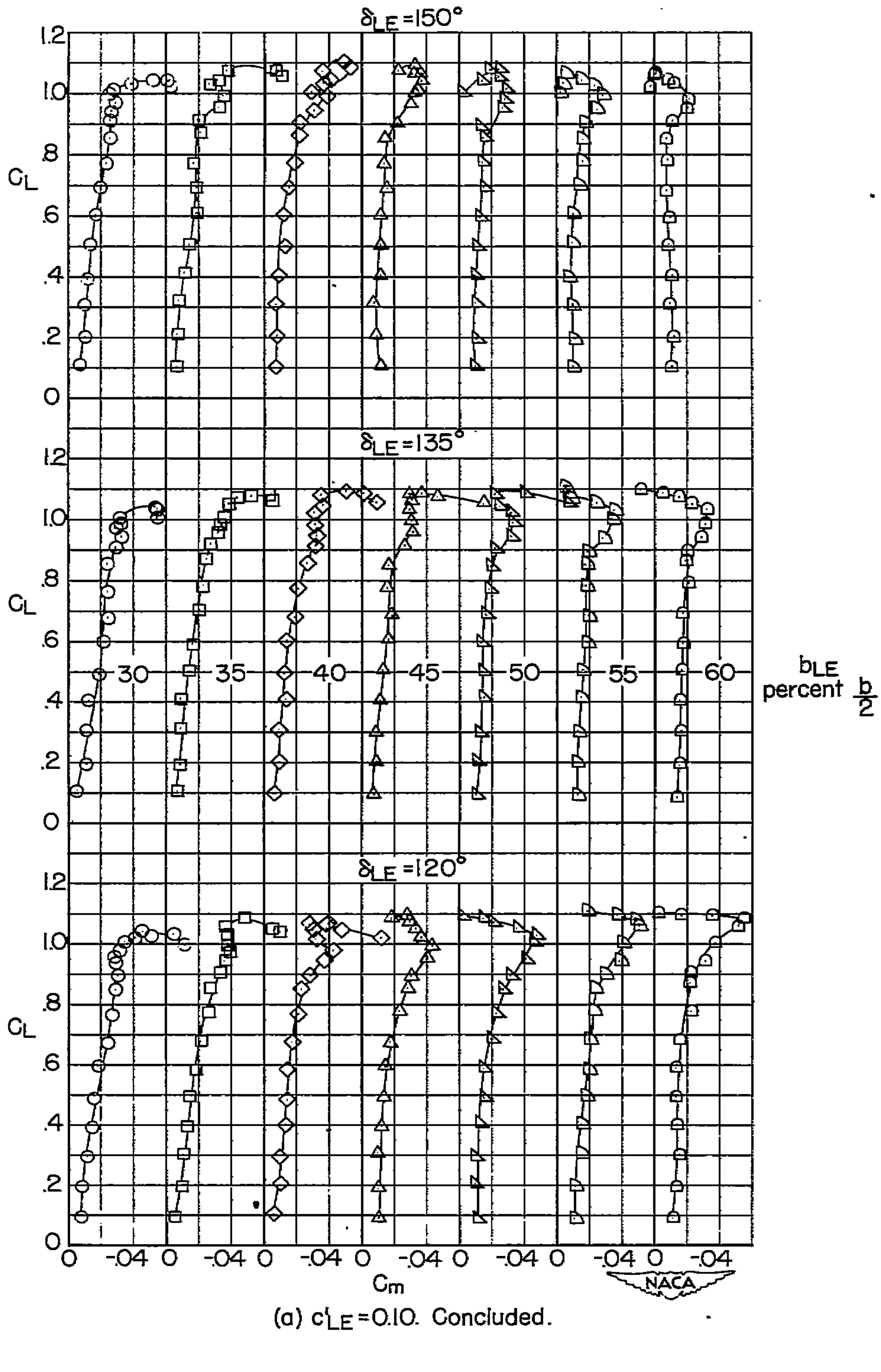

(a) c'_{LE} = 0.10. Concluded.

Figure 5.—Continued.

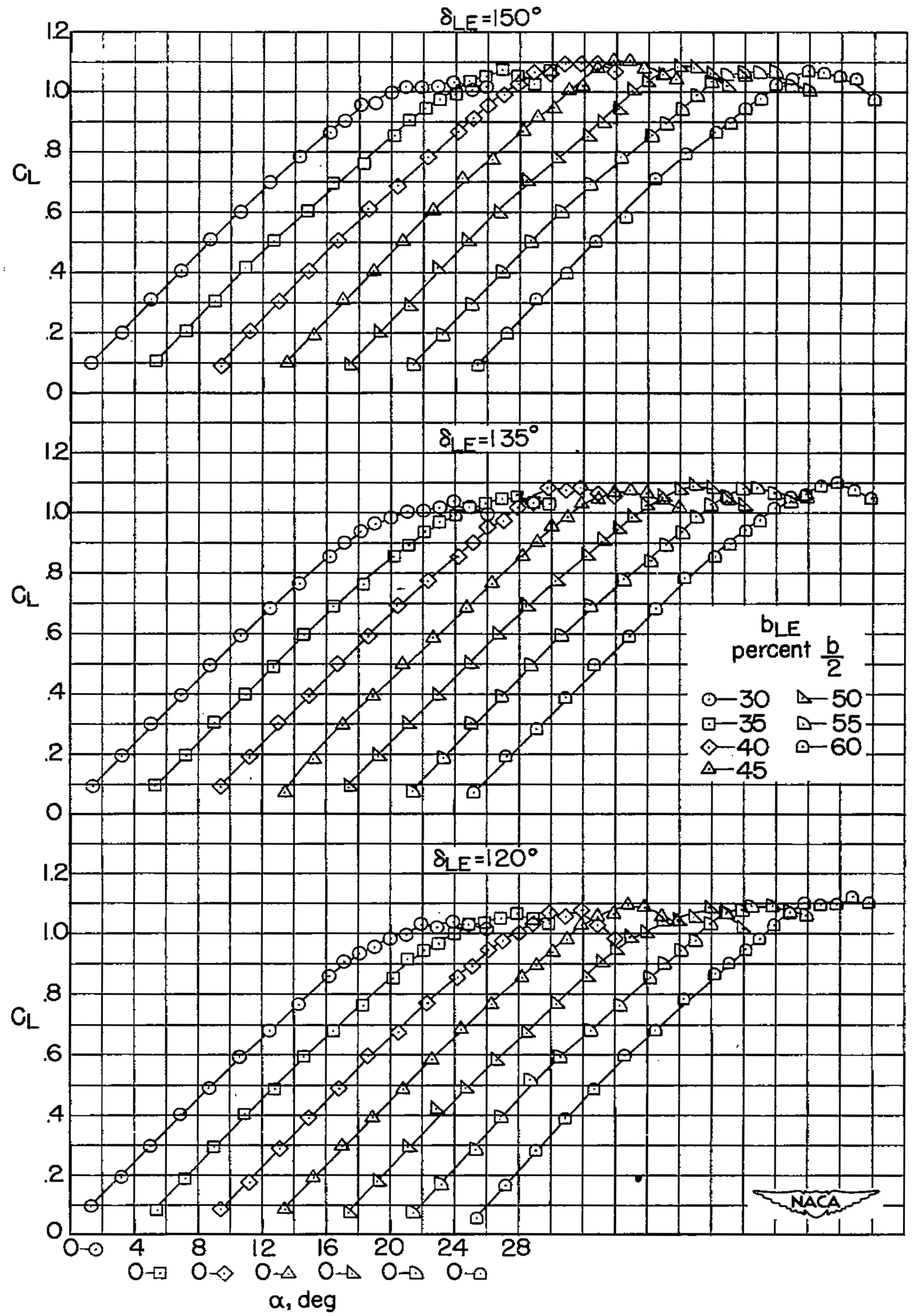

(b) c'_{LE} = 0.15.

Figure 5.-Continued.

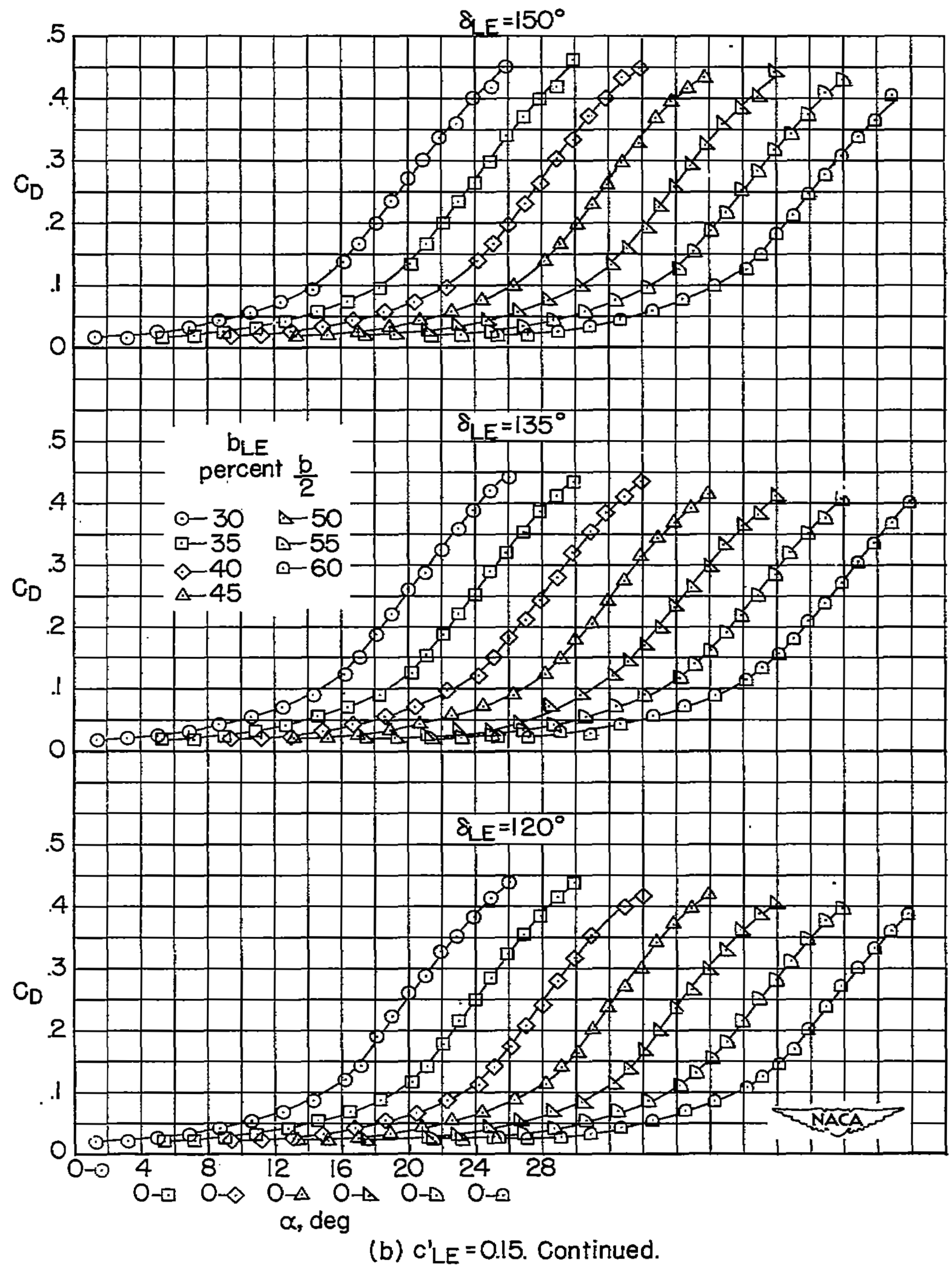

(b) c'_{LE} = 0.15. Continued.

Figure 5.—Continued.

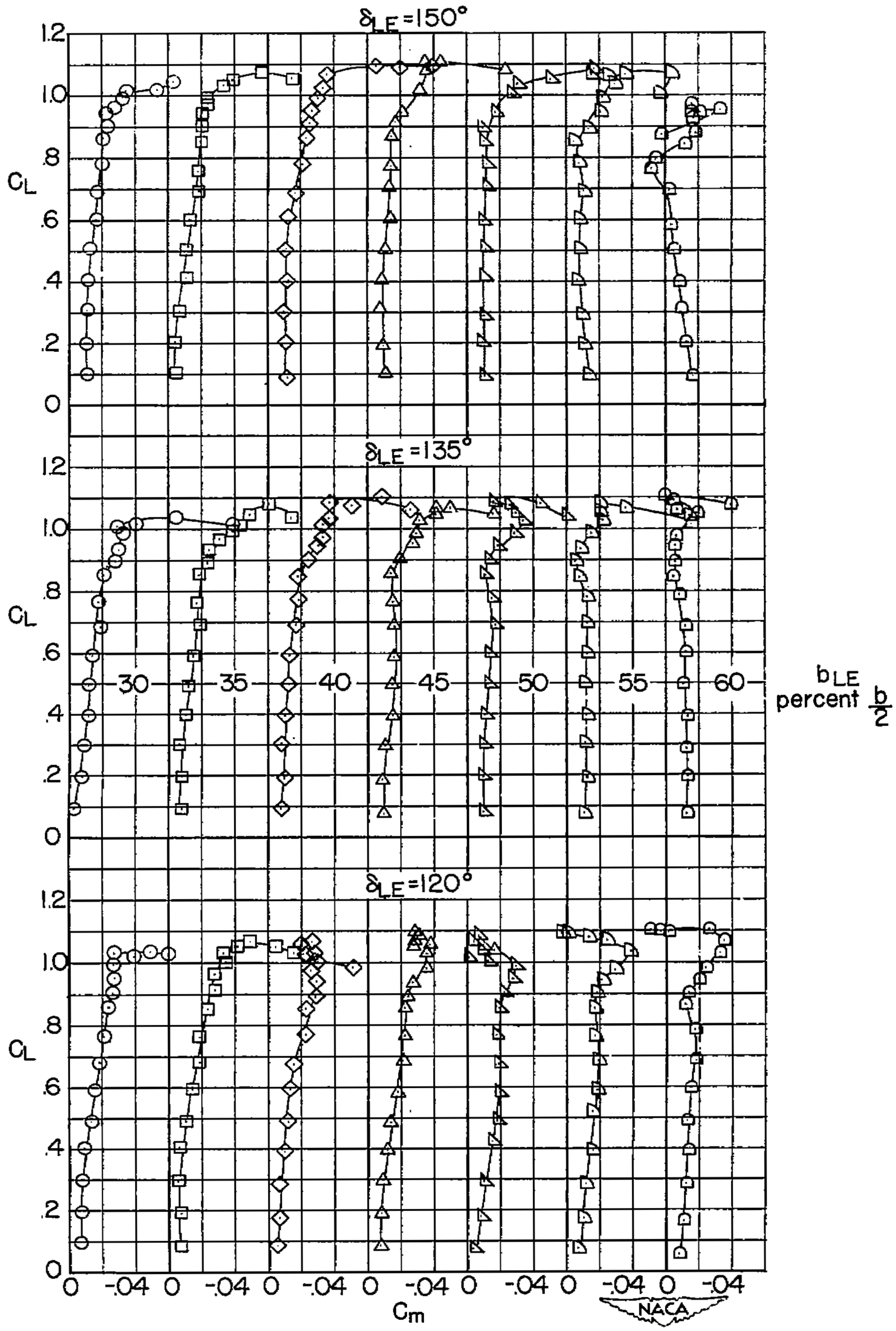

(b) c'_{LE} = 0.15. Concluded.

Figure 5.—Continued.

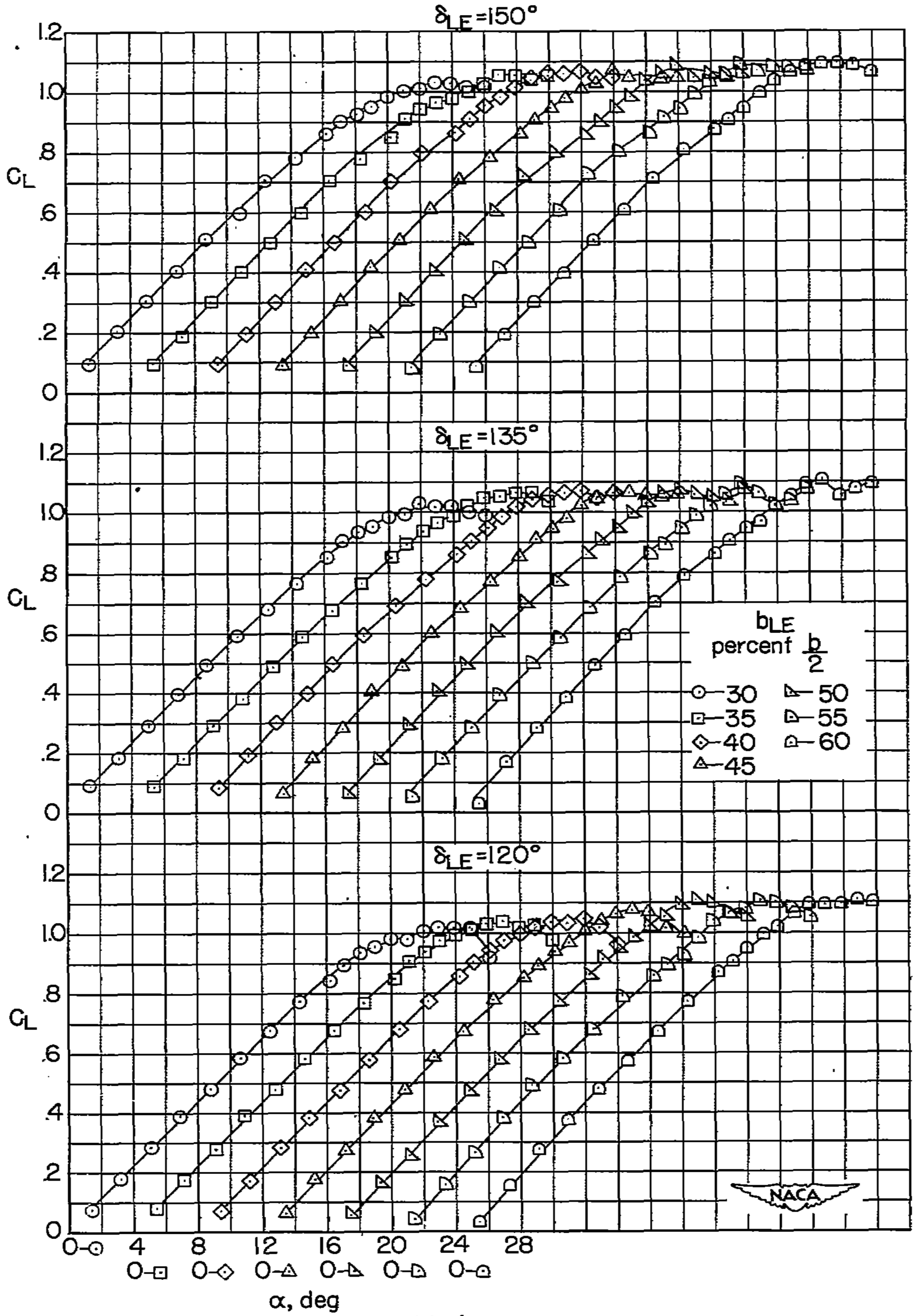

(c) c'_{LE} = 0.20.

Figure 5.–Continued.

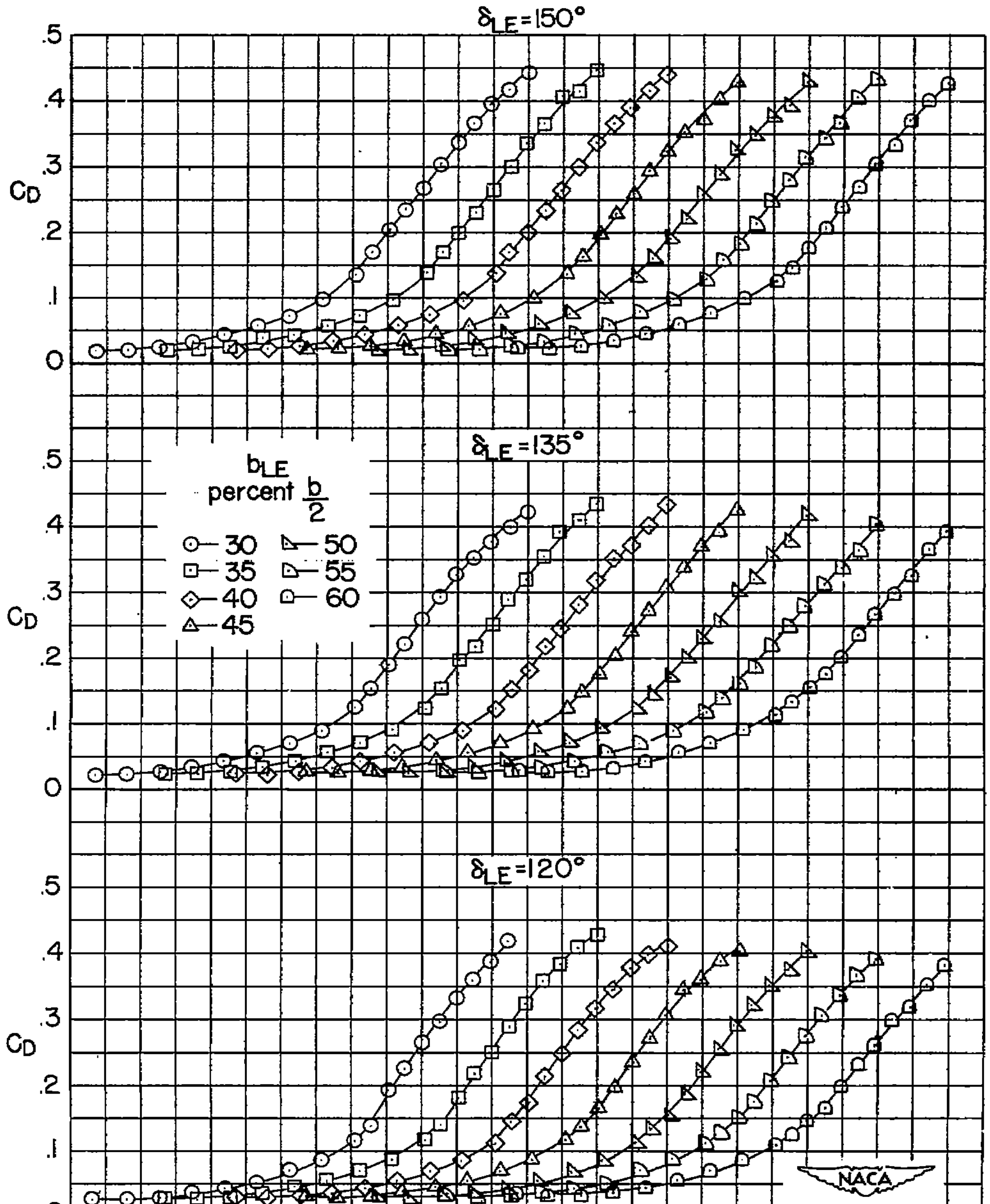

(c) c'_{LE} = 020. Continued.

Figure 5.—Continued.

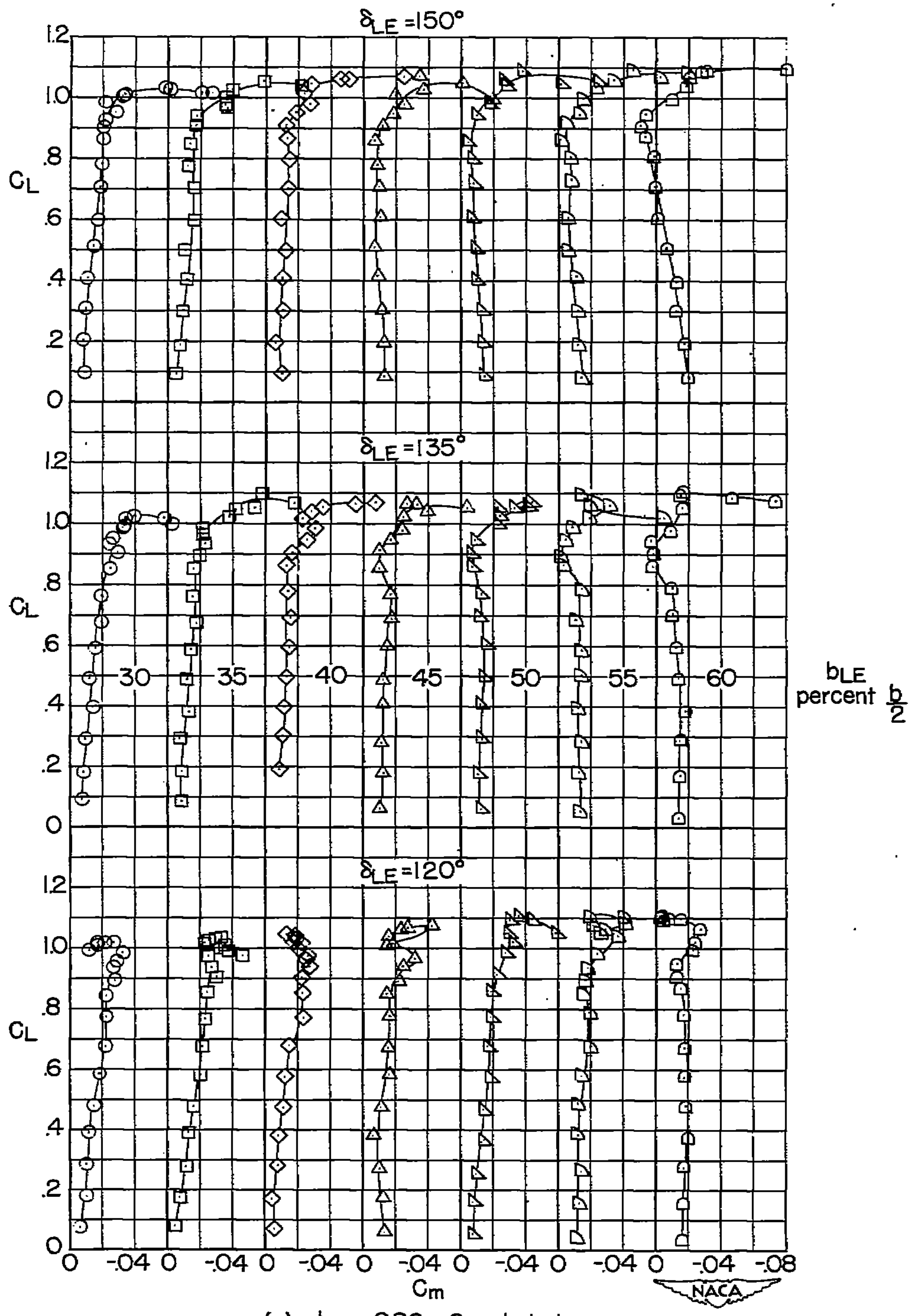

(c) c'_{LE} = 0.20. Concluded.

Figure 5.—Concluded.

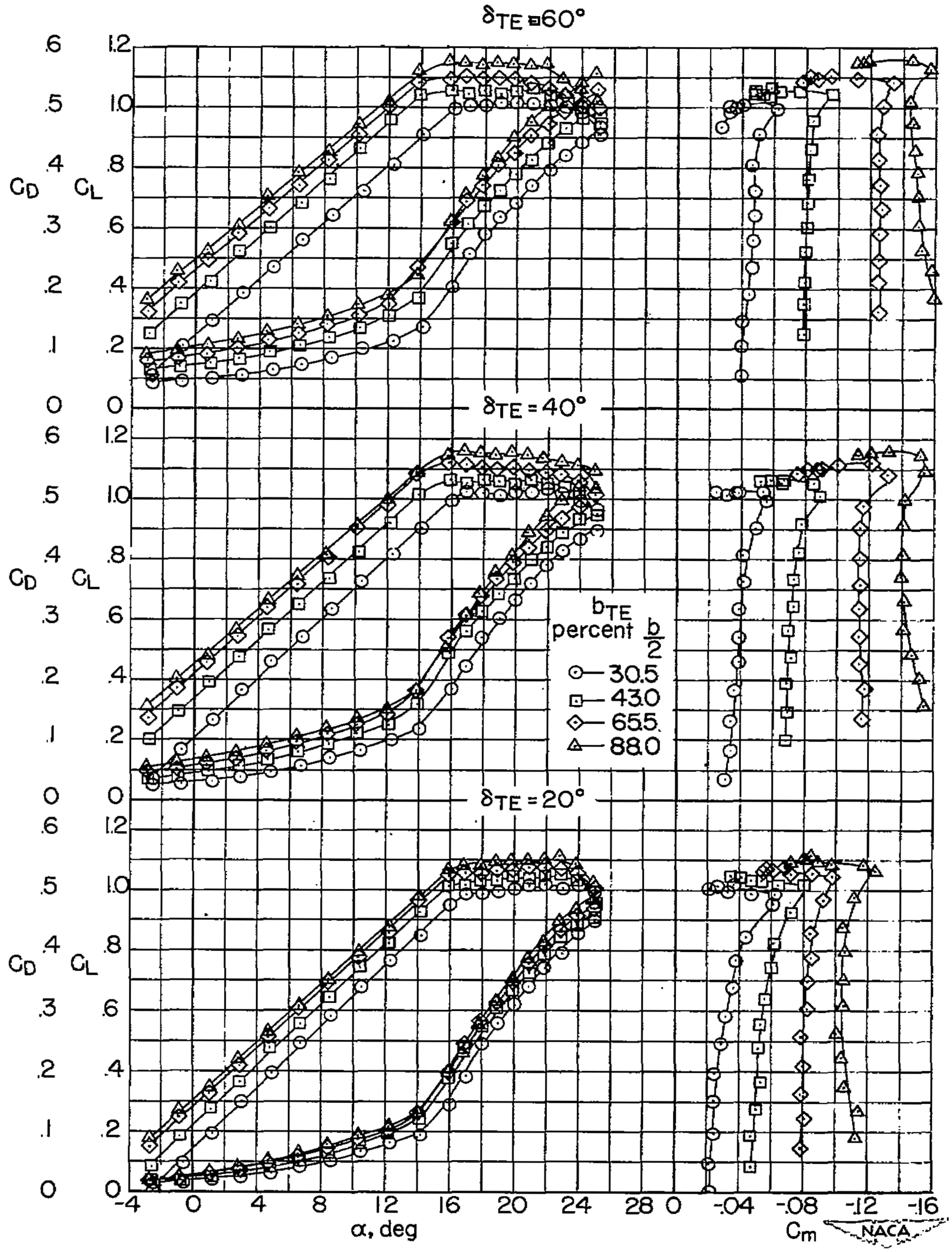

Figure 6.—Aerodynamic characteristics of a 47.5° sweptback wing-fuselage combination with plain trailing-edge flaps. $R = 4.4 \times 10^6$.

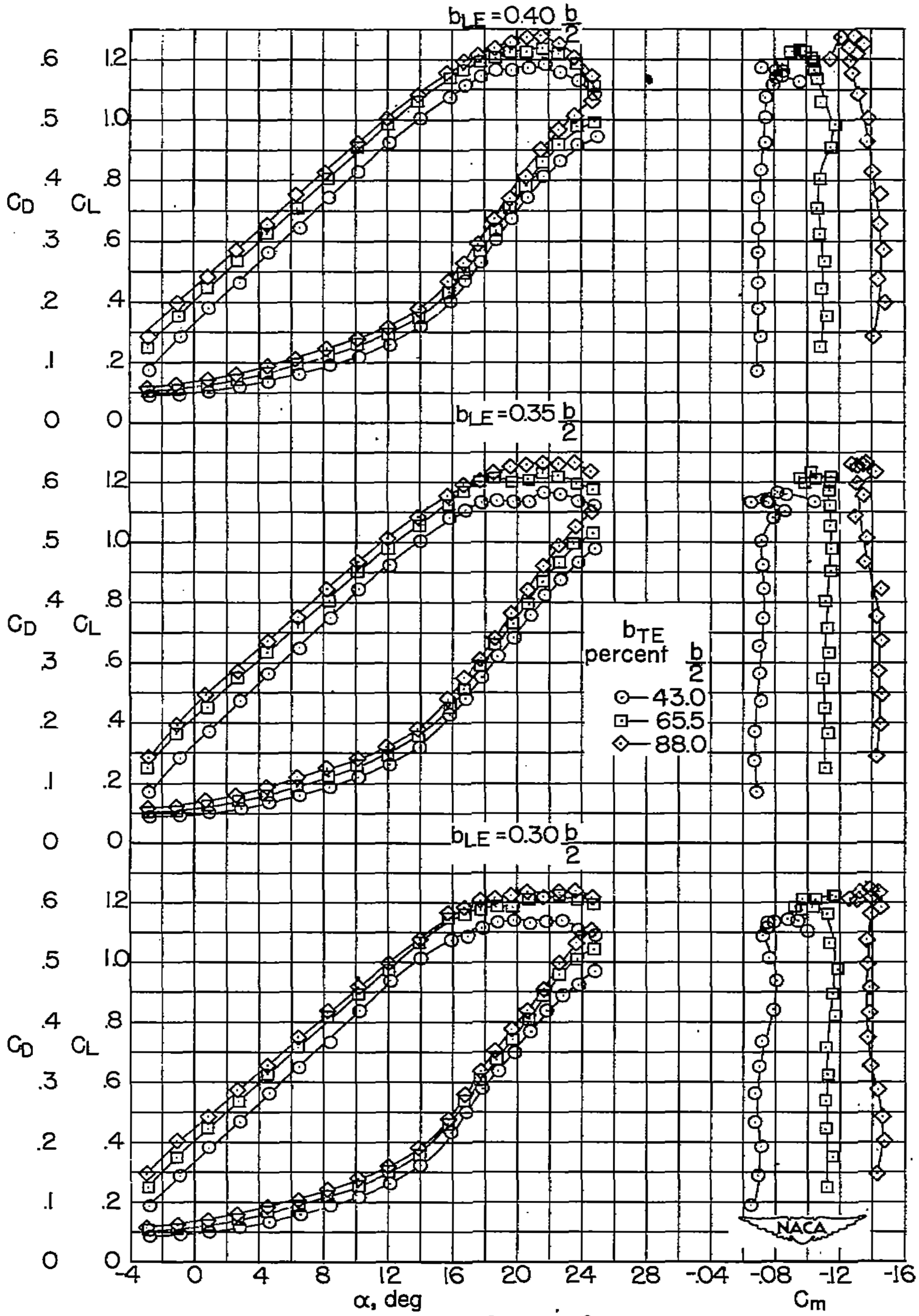

(a) $\delta_{LE} = 135°$.

Figure 7.—Aerodynamic characteristics of a 47.5° sweptback wing-fuselage combination with extensible leading-edge flaps and plain trailing-edge flaps. $c'_{LE} = 0.10$. $\delta_{TE} = 40°$. $R = 4.4 \times 10^6$.

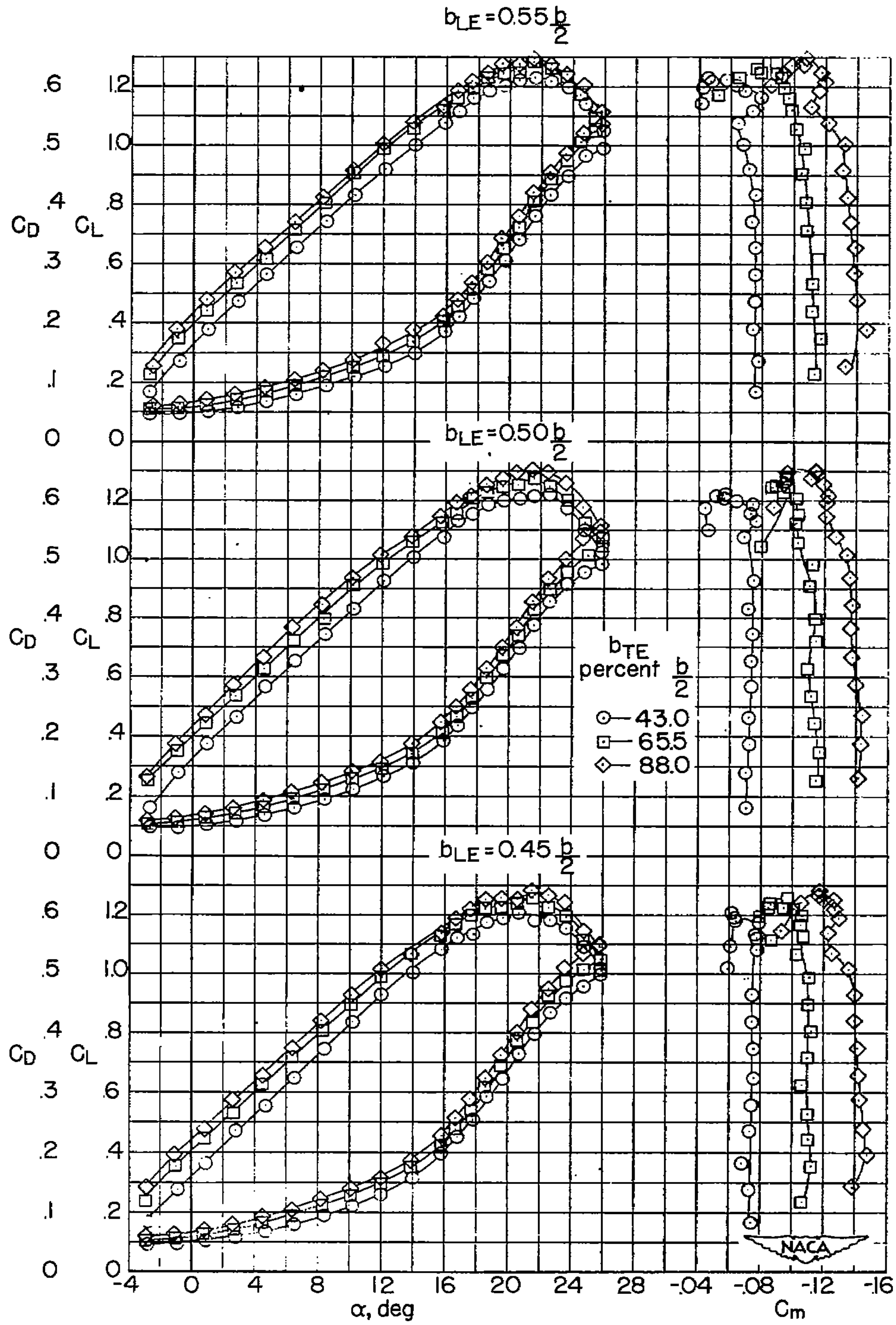

(a) $\delta_{LE} = 135^\circ$ Concluded.

Figure 7.—Continued.

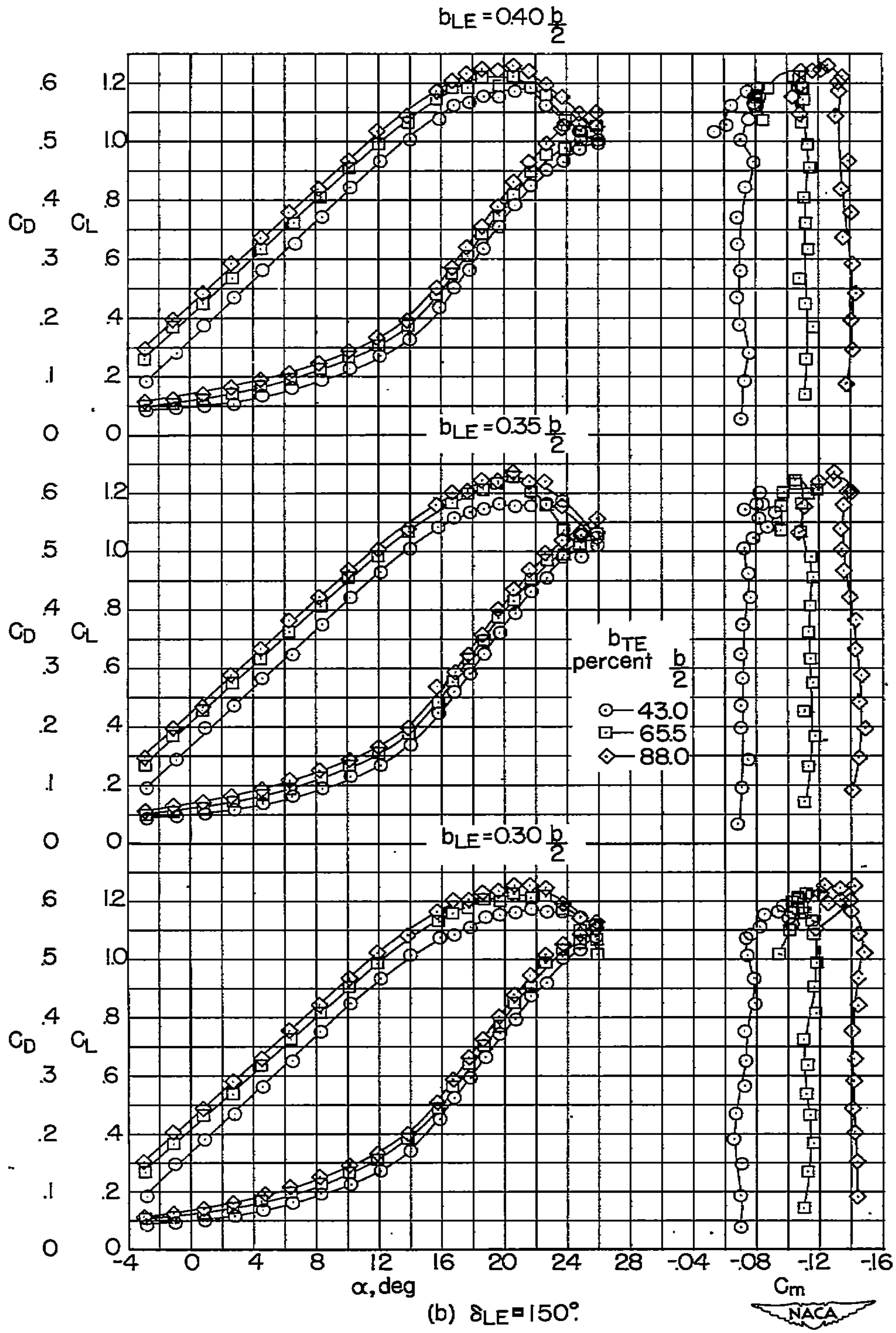

(b) $\delta_{LE} = 150°$.

Figure 7.—Continued.

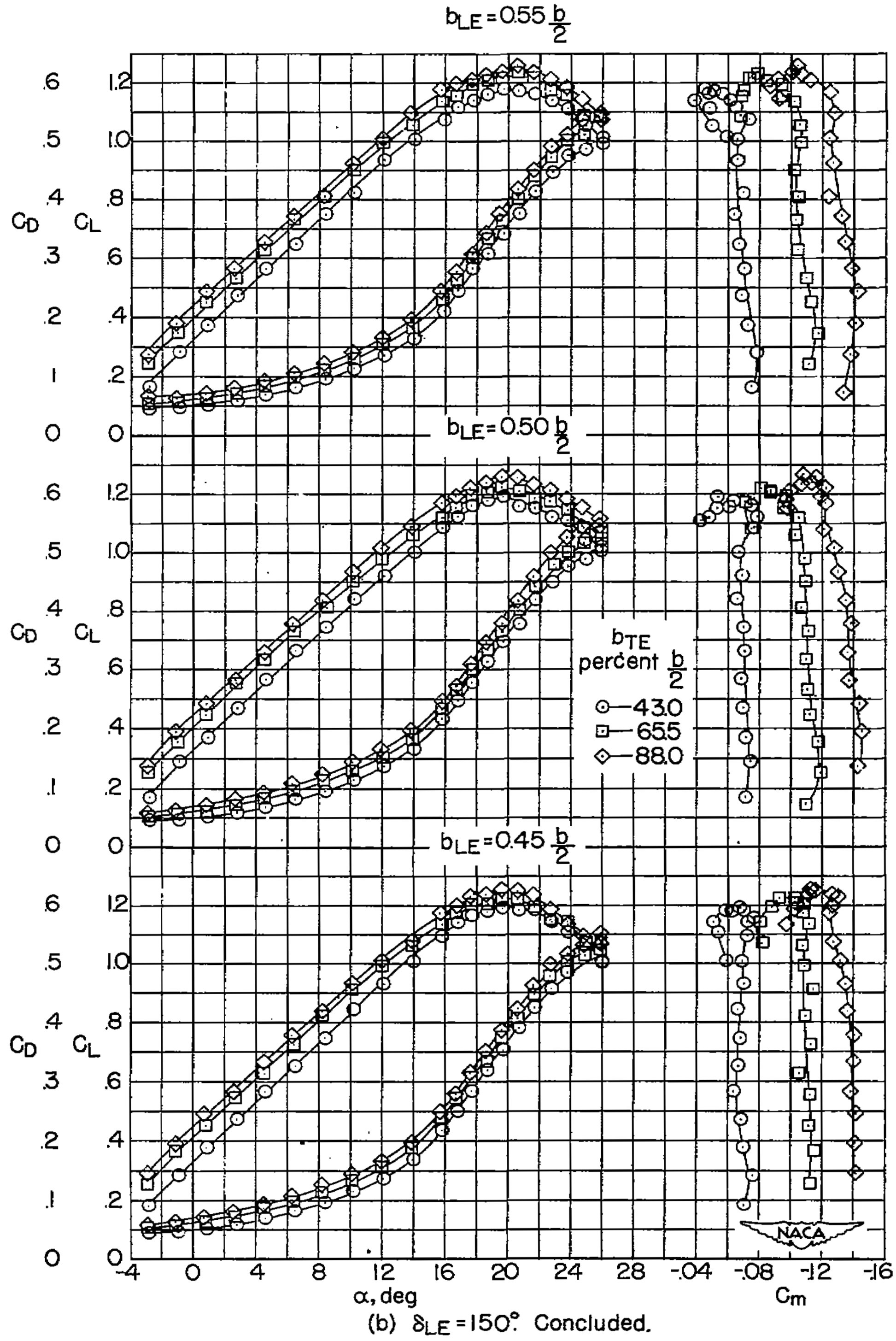

(b) $\delta_{LE} = 150°$. Concluded.

Figure 7.—Concluded.

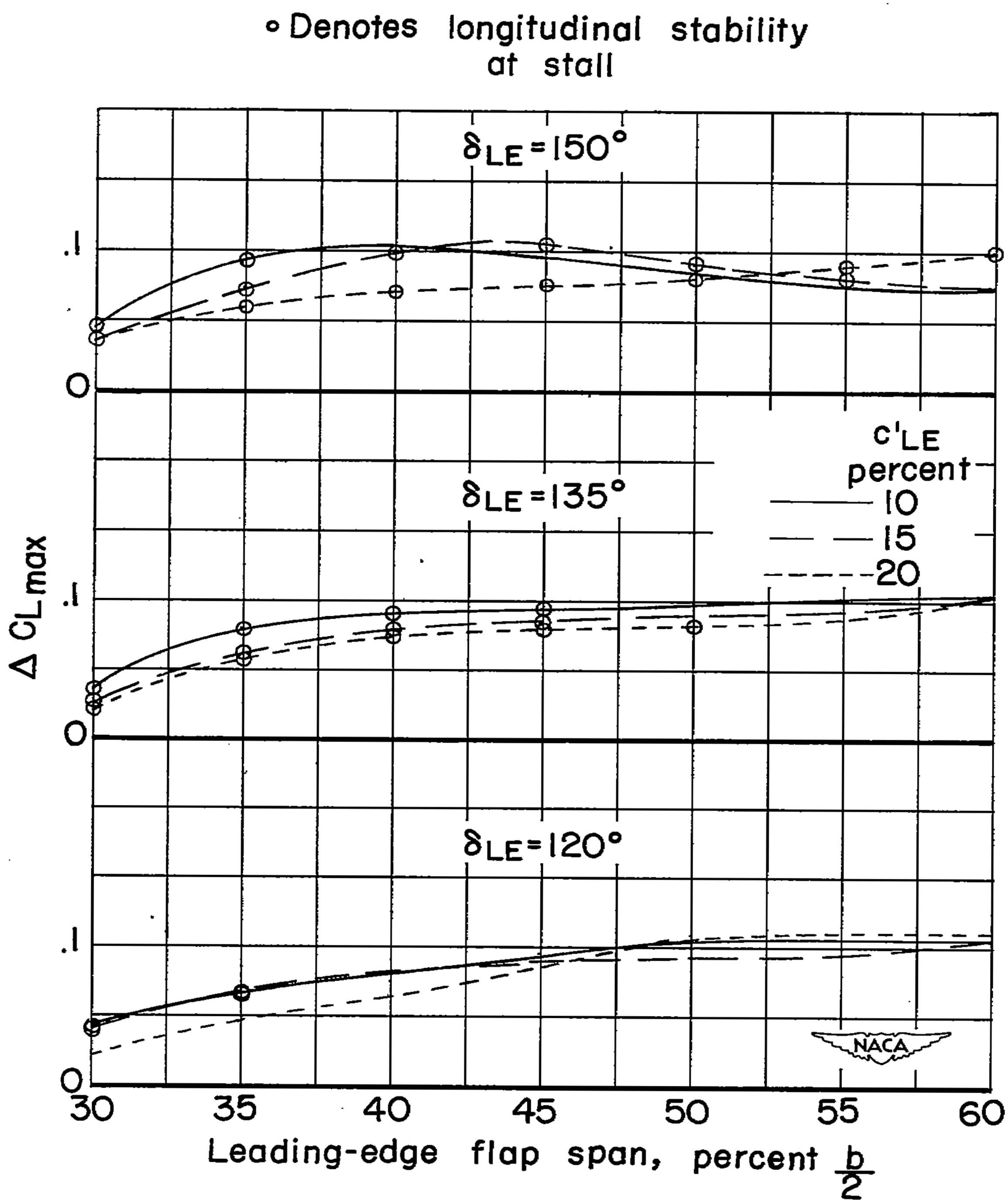

Figure 8.– Effect of extensible leading-edge flaps on the maximum lift of a 47.5° sweptback wing-fuselage combination. $R = 4.4 \times 10^6$.

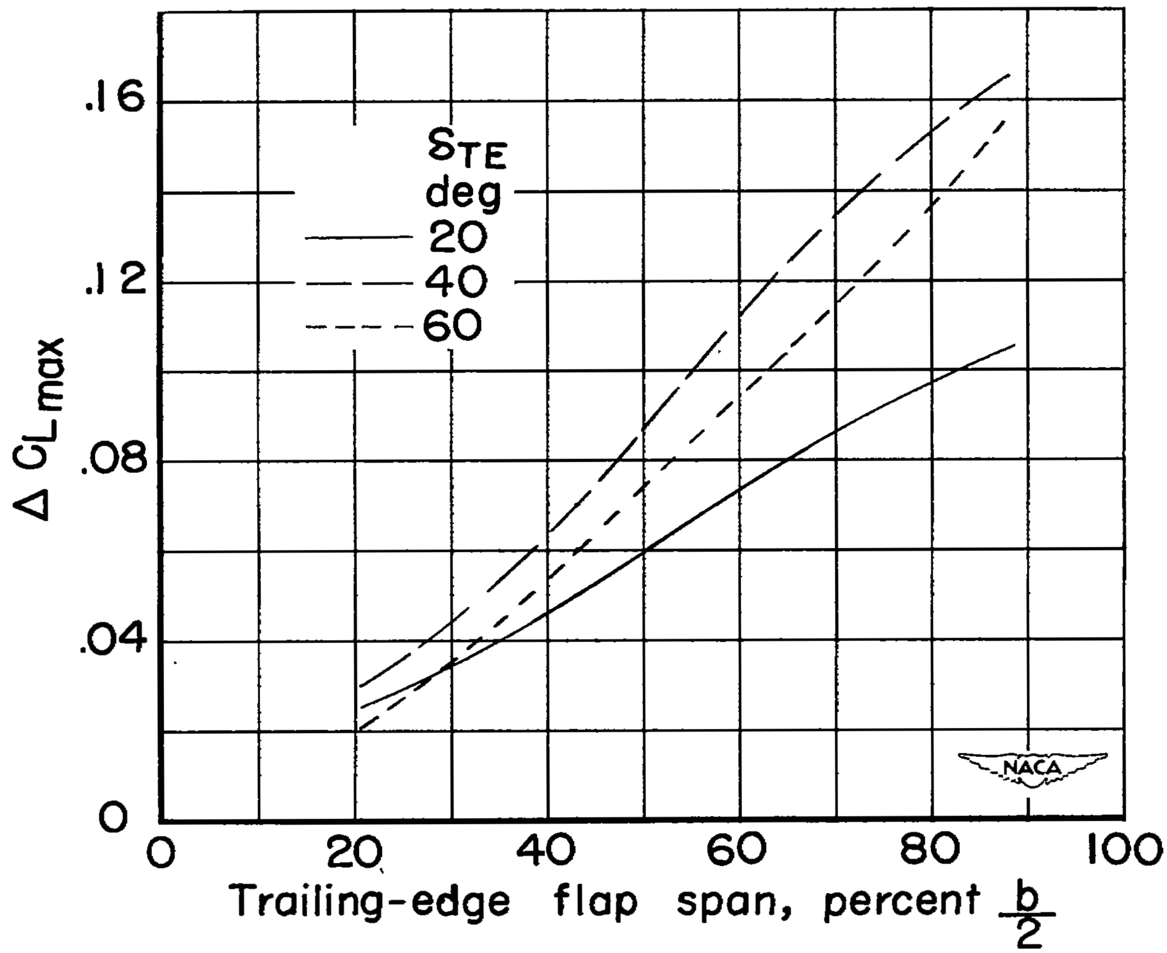

Figure 9.—Effect of plain trailing-edge flaps on the maximum lift of a 47.5° sweptback wing-fuselage combination. $R = 4.4 \times 10^6$.

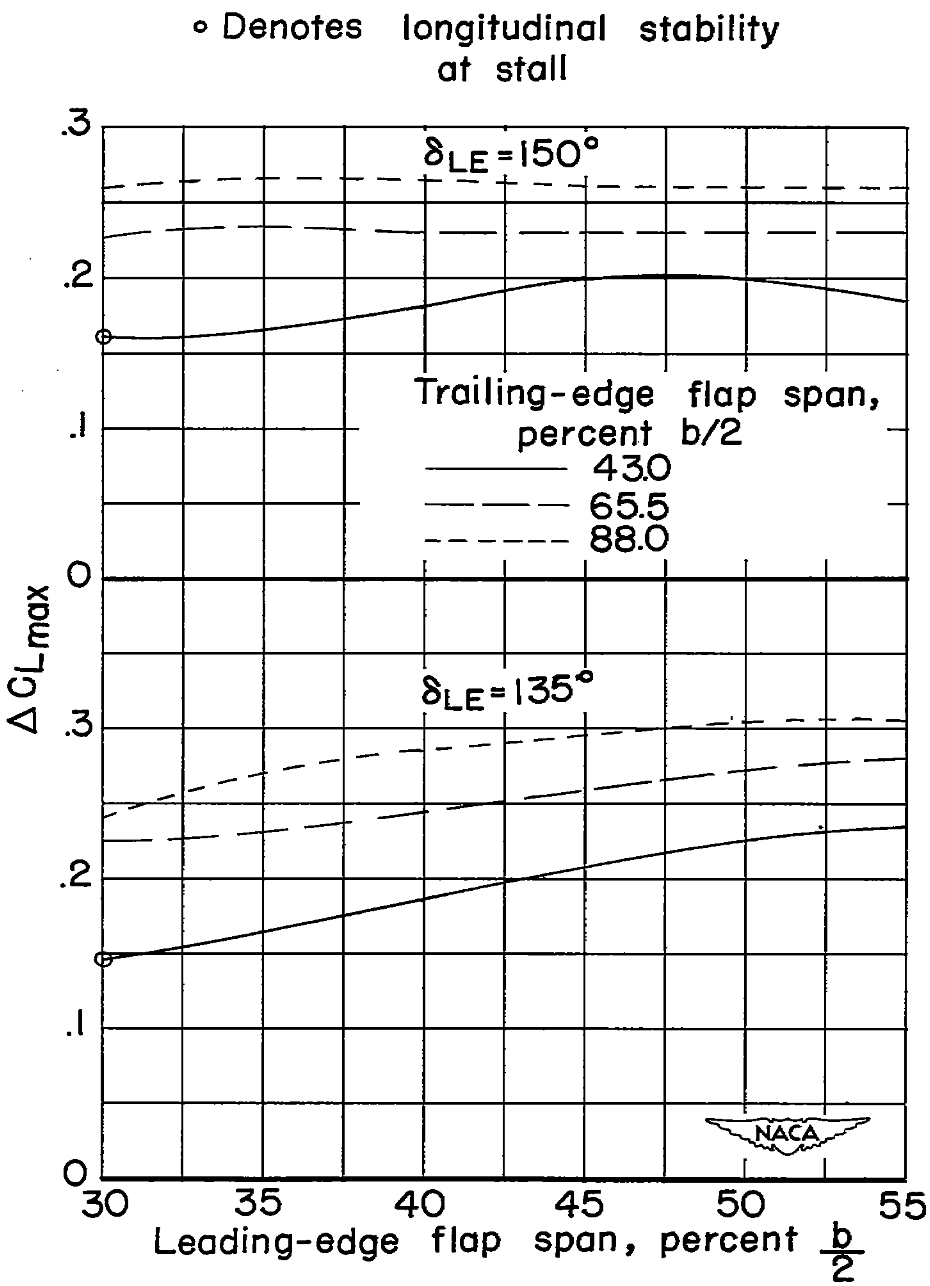

Figure 10.–Effect of combinations of extensible leading-edge flaps and plain trailing-edge flaps on the maximum lift of a 47.5° sweptback wing-fuselage combination. $\delta_{TE}=40°$. $c'_{LE}=0.10$. $R=4.4 \times 10^6$.